

1 **Estimation of temporal and spatial variations in**
2 **groundwater recharge in unconfined sand aquifers using**
3 **Scots pine inventories**

4
5 **P. Ala-aho¹, P.M. Rossi¹ and B. Kløve¹**

6
7 [1] Water Resources and Environmental Engineering Research Group, Faculty of Technology,
8 University of Oulu, P.O. Box 4300, 90014 University of Oulu, Finland

9 Correspondence to: P. Ala-aho (perti.ala-aho@oulu.fi)

10
11
12
13
14
15
16
17
18
19
20
21
22
23
24
25

26 **Abstract**

27 Climate change and land use are rapidly changing the amount and temporal distribution of
28 recharge in northern aquifers. This paper presents a novel method for distributing Monte Carlo
29 simulations of 1-D soil profile spatially to estimate transient recharge in an unconfined esker
30 aquifer. The modeling approach uses data-based estimates for the most important parameters
31 controlling the total amount (canopy cover) and timing (thickness of the unsaturated zone) of
32 groundwater recharge. Scots pine canopy was parameterized to leaf area index (LAI) using
33 forestry inventory data. Uncertainty in the parameters controlling soil hydraulic properties and
34 evapotranspiration was carried over from the Monte Carlo runs to the final recharge estimates.
35 Different mechanisms for lake, soil, and snow evaporation and transpiration were used in the
36 model set-up. Finally, the model output was validated with independent recharge estimates
37 using the water table fluctuation method and baseflow estimation. The results indicated that
38 LAI is important in controlling total recharge amount. Soil evaporation compensated for
39 transpiration for areas with low LAI values, which may be significant in optimal management
40 of forestry and recharge. Different forest management scenarios tested with the model showed
41 differences in annual recharge of up to 100 mm. The uncertainty in recharge estimates arising
42 from the simulation parameters was lower than the interannual variation caused by climate
43 conditions. It proved important to take unsaturated thickness and vegetation cover into account
44 when estimating spatially and temporally distributed recharge in sandy unconfined aquifers.

45

46

47

48

49

50

51

52

53

54 **1 Introduction**

55 Eskers are permeable, unconfined sand and gravel aquifers (Banerjee, 1975). In addition to
56 water supply, they support groundwater-dependent ecosystems and provide recreational
57 services (Kløve et al., 2011). Esker hydrology is important as eskers and other glaciofluvial
58 aquifer types cover large areas of the North and are among the dominant aquifer types in the
59 boreal zone. Management of these complex aquifers has gained recent attention (Bolduc et al.,
60 2005, Karjalainen et al., 2013, Koundouri et al., 2012, Kurki et al., 2013). The European
61 Groundwater Directive requires such systems to be characterized in order to determine their
62 quality status, so knowledge of how to estimate groundwater recharge in esker aquifers is
63 becoming increasingly important (EC, 2006). Esker aquifers are commonly covered with
64 managed pine forests, where the forest canopy is likely to influence recharge amounts. The soil
65 surface profile of eskers is complex and highly variable, consisting of kettle holes and sand
66 dunes, resulting in variable thickness of the unsaturated zone (Aartolahti, 1973), a factor which
67 also needs to be accounted for in recharge estimation.

68 Computational methods to estimate groundwater recharge vary from simple water balance
69 models, where water stores and fluxes are represented conceptually and related with adjustable
70 parameters (Jyrkama et al., 2002), to physically-based models using the Richards equation
71 (Assefa and Woodbury, 2013, Okkonen and Kløve, 2011) to solve water fluxes through
72 unsaturated zone. Computational methods solving the Richards equation are often limited to
73 small-scale areal simulations (Scanlon et al., 2002a) and shallow unsaturated zones, and they
74 commonly lack the soil freeze, thaw, and snow storage sub-routines relevant at higher northerly
75 latitudes (Okkonen, 2011). However, computational approaches can be employed to produce
76 the values on spatial and temporal variability in recharge often needed in groundwater modeling
77 (Dripps and Bradbury, 2010). The methods commonly rely on a GIS platform for spatial
78 representation and calculation approaches based on water balance to create the temporal
79 dimension of recharge (Croteau et al., 2010, Dripps and Bradbury, 2007, Jyrkama et al., 2002,
80 Sophocleous, 2000, Westenbroeck et al., 2010). Neglecting variations in thickness of the
81 unsaturated zone is common practice in many water balance models used in recharge
82 estimations. However, the residence time in the unsaturated zone may play an important role,
83 especially in the timing of recharge in deep unsaturated zones (Hunt et al., 2008), as
84 acknowledged in recent work (Assefa and Woodbury, 2013, Jyrkama and Sykes, 2007, Scibek
85 and Allen, 2006, Smerdon et al., 2008).

86 In numerical recharge models, actual evapotranspiration (ET) is a difficult variable to estimate
87 accurately from climate, soil, and land use data. The vegetation is commonly parameterized
88 from land use or land cover maps (Assefa and Woodbury, 2013, Jyrkama et al., 2002, Jyrkama
89 and Sykes, 2007, Keese et al., 2005), where the vegetation characteristics and leaf area index
90 (LAI) are estimated based solely on vegetation type. In addition to tree canopy transpiration,
91 soil evaporation, i.e. evaporation from the pores of soil matrix, can constitute a large proportion
92 of total ET. Soil evaporation from the forest floor is generally reported to range from 3 to 40%
93 of total ET (Kelliher et al., 1993), although values as high as 92% have been recorded (Kelliher
94 et al., 1998). For conifer forest canopies, soil evaporation can largely compensate for low
95 transpiration in areas with lower LAI (Ohta et al., 2001, Vesala et al., 2005). Data on canopy-
96 scale evaporation rates at latitudes above 60°N are rare (Kelliher et al., 1993). A few studies
97 have estimated ET from pine tree stands at patch scale (Kelliher et al., 1998, Lindroth, 1985),
98 but none has extended this analysis to spatially distributed groundwater recharge. Forest
99 management practices have the potential to affect the transpiration characteristics of coniferous
100 forests, which typically leads to increased groundwater recharge (Bent, 2001, Lagergren et al.,
101 2008, Rothacher, 1970).

102 The overall aim of the study was to provide novel information on groundwater recharge rates
103 and factors contributing to the amount, timing, and uncertainty of groundwater recharge in
104 unconfined sandy eskers aquifers. Study expands the application of physically-based 1-D
105 unsaturated water flow modeling for groundwater recharge, while taking into account detailed
106 information on vegetation (pine, lichen), unsaturated layer thickness, cold climate, and
107 simulation parameter uncertainty. Furthermore, this study considers the effect that forestry land
108 use has on vegetation parameters and how this is reflected in groundwater recharge.

109

110 **2 Materials and Methods**

111 **2.1 Study site**

112 Groundwater recharge was estimated for the case of the Rokua esker aquifer in northern Finland
113 (Fig. 1). Rokua is an unconfined aquifer consisting of unconsolidated sandy sediments (from
114 here on referred to as soil) underlain by crystalline bedrock (Fig. 2). Aquifer was formed
115 during previous deglaciation when rivers under the melting ice sheet deposited sandy sediments
116 in the river bed (Aartolahti 1973). The Rokua esker has a rolling surface topography in the

117 aquifer recharge area rising about 60 m above the flat peatland areas surrounding the esker. In
118 the groundwater discharge areas, the aquifer is locally confined by peat soil with low hydraulic
119 conductivity (Rossi et al. 2012).

120 The climate at the Rokua aquifer is characterized by precipitation exceeding evapotranspiration
121 on an annual basis and statistics of the annual climate for the study period 1961 - 2010 in terms
122 of precipitation, air temperature and FAO reference evapotranspiration according to Allen et al.
123 (1998) is presented in Table 1. Another important feature of the climate is annually recurring
124 winter periods when most precipitation is accumulated as snow.

125 2.1.1 Leaf area index from forestry inventories

126 Forestry inventory data from the Finnish Forest Administration (Metsähallitus, MH) and
127 Finnish Forest Centre (Metsäkeskus, MK) were used to estimate LAI for the Rokua esker
128 groundwater recharge area. The available data consisted of 2786 individual plots covering an
129 area of 52.4 km² (62.4% of the model domain). The forestry inventories, performed mainly
130 during 2000-2011, showed that Scots pine (*Pinus sylvestris*) is the dominant tree in the model
131 area (94.2% of plots). The forest inventory data include a number of data attributes and the
132 following data fields, included in both the MH and MK datasets, were used in the analysis:

- 133 - Plot area (p_A); [ha]
- 134 - Main canopy type
- 135 - Average tree stand height (h); [m]
- 136 - Average stand diameter at breast height (d_{bh}); [cm]
- 137 - Number of stems (n_{stm}); [1 ha^{-1}]
- 138 - Stand base area (b_A); [$\text{m}^2 \text{ ha}^{-1}$]
- 139 - Stand total volume (V); [m^3]

140 Inventory plots were excluded from the analysis if: (1) main canopy type was not pine forest,
141 (2) data were missing for d_{bh} and h or n_{stm} , or (3) the MH and MK datasets overlapped, in which
142 case MH was retained. However, several plots in the MH dataset were lacking n_{stm} data, which
143 would have created a large gap in data coverage. Therefore the n_{stm} variable was estimated with
144 a log-transformed regression equation using data on d_{bh} , p_A , and V as independent variables.
145 This regression equation was built from 280 plots ($R^2 = 0.88$) and used to estimate n_{stm} for 288

146 plots. LAI was estimated as described by Koivusalo et al. (2008). Needle mass for an average
147 tree in stand/plot was estimated from h and d_{bh} using empirical equations presented by Repola
148 et al. (2007). LAI for a stand was calculated as:

$$149 \quad LAI = N_t * n_{stm} * S_{LA} \quad (1)$$

150 where N_t = needle mass per average tree in stand [kg], n_{stm} = number of stems per hectare
151 [1 ha^{-1}], and S_{LA} = specific leaf area = $4.43 \text{ m}^2 \text{ kg}^{-1} = 4.43 * 10^{-4} \text{ ha kg}^{-1}$ (Xiao et al., 2006).

152 Detailed information on LAI was used to obtain an estimate of how different forest management
153 options, already actively in operation in the area, could potentially affect groundwater recharge.
154 Three scenarios were simulated testing the potential impact of forestry operations on
155 groundwater recharge:

- 156 1) The first “baseline” scenario simulated the current situation by using LAI pattern at
157 the site (Fig. 3) estimated with Eq. (1).
- 158 2) The second scenario simulated the impact of intensive forestry operations as clear-
159 cutting of the tree stand. Clear-cutting is an intensive land use form where almost the
160 entire tree stand is removed, and it is carried out in some parts of the study area. Low
161 LAI values of 0-0.2 for the whole study site were used in simulating this scenario.
- 162 3) The third scenario simulated the impact of no forestry operations, i.e. absence of
163 forestry cuttings. The hypothetical mature stand covering the study site was assumed
164 to have high LAI values of 3.2-3.5 found at the study site and reported in the literature
165 (Koivusalo et al., 2008, Rautiainen et al., 2012, Vincke and Thiry, 2008, Wang et al.,
166 2004).

167 2.1.2 Lichen water retention

168 An organic lichen layer covers much of the sandy soil at the Rokua study site (Kumpula et al.,
169 2000), so this lichen layer was introduced in soil evaporation (SE) calculations. Although
170 lichens do not transpire water, their structural properties allow water storage in the lichen matrix
171 and capillary water uptake from the soil (Blum, 1973, Larson, 1979). In this study, water
172 interception storage by the lichen layer was estimated from lichen samples. In total, six samples

173 (species *Cladonia stellaris* and *C. rangiferina*) were taken in May 2011 from two locations 500
174 m apart, close to borehole MEA506 (see Fig. 1). These samples were collected by pressing
175 plastic cylinders (diameter 10.6 cm) through the lichen layer and extracting intact cores, after
176 which mineral soil was carefully removed from the base of the sample. Thus the final sample
177 consisted of a lichen layer on top and a layer of organic litter and decomposed lichen at the
178 bottom, and was sealed in a plastic bag for transportation. To obtain estimates of water retention
179 capacity, the samples were first wetted until saturation with a sprinkler, left overnight at +4 °C
180 to allow gravitational drainage and weighed to determine ‘field capacity’. The samples were
181 then allowed to dry at room temperature and weighed daily until stable final weight (‘dry
182 weight’) was reached. The water retention capacity (w_r) of the sample was calculated as:

$$183 \quad w_r = \frac{m_{fc} - m_{dry}}{\rho_w} \cdot \frac{1}{\pi \cdot r^2} \quad (2)$$

184 where m_{fc} is the field capacity weight [M], m_{dry} is the final dry weight [M] at room temperature,
185 ρ_w [M L⁻³] is the density of water, and r [L] is the radius of the sampling cylinder.

186 The mean water retention capacity of the lichen samples was found to be 9.85 mm (standard
187 deviation (SD) 2.71 mm) and approximations for these values were used in model
188 parameterization (Table 2). To acknowledge the lack of information about (B&C) parameter
189 estimates for lichen, the parameters were included in the simulations Monte Carlo runs (see
190 section 2.2.1) with ranges which in our opinion produced reasonable shape of the pressure-
191 saturation curve allowing easy drainage of the lichen.

192 2.1.3 Soil hydraulic properties

193 Soil texture was determined by sieving (ISO 3310-1 standard sieve, US sieve numbers 5, 10,
194 18, 35, 60, 120, and 230) 26 soil samples taken from five boreholes at various depths (Fig. 1).
195 14 of the samples were analyzed also for pressure saturation curves. Samples were characterized
196 as fine or medium sand, while soil texture in the other boreholes (Fig. 1) had previously been
197 characterized as medium, fine or silty sand throughout the model domain by the Finnish
198 Environmental Administration as expert *in-situ* analysis during borehole drilling. Therefore the
199 soil samples from the five boreholes were considered to be representative of the soil type in the
200 area. Pressure saturation data from the samples was then used to define parameter ranges for
201 the Brooks and Corey equation used in the simulations (Table 2). Furthermore, texture values
202 were employed to calculate the range of saturated vertical hydraulic conductivity for the
203 samples, using empirical equations by Hazen, Kozeny-Carman, Breyer, Slitcher, and Terzaghi

204 (Odong, 2007). The hydraulic conductivity for a given sample ranged approximately one order
205 of magnitude between the equations. When using the five equations for the 26 samples in total,
206 the calculated values were within $1.99 \cdot 10^{-5} - 1.47 \cdot 10^{-3}$ [m s^{-1}] for all but one sample. The
207 obtained range was considered to reasonably represent the hydraulic conductivity variability in
208 the study area and simulations.

209 2.1.4 Climate data

210 Driving climate data for the model were taken from Finnish Meteorological Institute databases
211 for the modeling period 1 Jan 1961-31 Oct 2010. Daily mean temperature [$^{\circ}\text{C}$] and sum of
212 precipitation [mm] were recorded at Pelso climate station, 6 km south of the study area (Fig.
213 1). The most representative long-term global radiation data [$\text{kJ m}^{-2} \text{d}^{-1}$] for the area were
214 available as interpolated values in a 10 x 10 km grid covering the whole of Finland. The
215 interpolation data point was found to be at approximately the same location as borehole
216 MEA2110 (Fig. 1). Long-term data on wind speed [m s^{-1}] and relative humidity [%] were taken
217 from Oulunsalo and Kajaani airports, located 60 and 40 km from the study site, respectively.
218 The data from the airports were instantaneous observations at three-hour intervals, from which
219 daily mean values were calculated. All the climate variables were recorded at reference height
220 2 m except for wind speed, which was measured at 10 m height. The wind speed data were
221 therefore recalculated to correspond to 2 m measurement height according Allen et al. (1998)
222 by multiplying daily average wind speed by 0.748. The suitability of long-term climate data for
223 the study site conditions was verified with observations made at a climate station established at
224 the study site in an overlapping time period (Dec 2009-Oct 2010) and the agreement between
225 the measurements was found to be satisfactory.

226 Data on long-term lake surface water temperature were needed to calculate lake evaporation
227 (see section 2.2.3), but were not available directly at the study site. However, surface water
228 temperature was recorded at Lake Oulujärvi by the Finnish environmental administration
229 (2013) 22 km from the study site in the direction of the Kajaani climate station (Fig. 1). The
230 Oulujärvi water temperature was found to be closely correlated (linear correlation coefficient
231 0.97) with daily lake water temperature recorded at Rokua during summer 2012. Daily lake
232 surface temperature data for Lake Oulujärvi starting from 21 July 1970 were used in lake
233 evaporation modeling. However, the data series had missing values for early spring and some
234 gaps during five years in the observation period. These missing values were estimated with a

235 sine function, corresponding to the average annual lake temperature cycle, and a daily time
236 series was established for subsequent calculations.

237 Snowmelt was calculated with a degree-day approach model in Jansson and Karlberg (2004).
238 Snow routines were calibrated separately using bi-weekly snow water equivalent (SWE) data
239 from Vaala snowline measurements (Finnish environment administration, 2011) for the period
240 1960-2010 (Fig. 1). This separately calibrated snow model was used for all subsequent
241 simulations.

242 **2.2 Recharge modeling framework**

243 **2.2.1 Water flow simulation in 1-D unsaturated soil profile**

244 Water flow through an unsaturated one-dimensional (1-D) sandy soil profile (Fig. 2) was
245 estimated with the Richards equation using CoupModel (Jansson and Karlberg, 2004).
246 CoupModel was selected as the simulation code because of its ability to represent the full soil-
247 plant-atmosphere continuum adequately and to include snow processes in the simulations
248 (Okkonen and Kløve, 2011). The simulated soil profile was vertically discretized into 61 layers
249 with increasing layer thickness deeper in the profile. Layer thickness was 0.1 m for the first 16
250 layers (until 1.6 m), where the topmost 0.1 m was represented as a lichen layer. Layer thickness
251 was progressively increased by defining 0.2 m thickness for the next 7 layers (between 1.6 and
252 3 m), 0.5 m for the next 14 layers (between 3 and 10 m), 1 m for the next 7 layers (between 10
253 and 17 m) and 2 m for last 17 layers ranging from 17 m to the bottom of the profile (51 m).

254 The time variable boundary condition for water flow at the top of the column was defined by
255 driving climate variables and affected by sub-routines accounting for snow processes with daily
256 time step. The short time step was chosen to fully capture the main recharge input from
257 snowmelt. All water at the top of the domain was assumed to be subjected to infiltration. Deep
258 percolation as gravitational drainage was allowed from soil column base using the unit-gradient
259 boundary condition (see e.g. Scanlon et al., 2002b). Simulations for the unsaturated 1-D soil
260 profile were made for the period 1970-2010, and before each run 10 years of data (1960-1970)
261 were used to spin up the model.

262 The simulation of the 1-D soil profile was performed 400 times as Monte Carlo runs to facilitate
263 the propagation of model parameter uncertainty in the final model output. Model was ran each
264 time with different parameter values as specified in Table 2. For each individual simulation

265 homogeneity in the vertical direction in terms of soil hydraulic properties was assumed. The
266 parameters for which values were randomly varied were chosen beforehand by trial and error
267 model runs exploring the sensitivity of parameters with respect to cumulative recharge or
268 evapotranspiration. The parameter ranges were specified from field data when possible;
269 otherwise we resorted to literature estimates or in some cases used $\pm 50\%$ of the CoupModel
270 default providing a typical parameter for the used equation.

271 The sensitivity of the parameters varied in the simulations was tested with Kendall correlation
272 analysis, by testing the correlation between each model parameter and cumulative sums of
273 different evapotranspiration components and soil infiltration for the 400 model runs. Individual
274 simulation with unique parameter values did not produce a groundwater recharge value due to
275 the assembling strategy for recharge; therefore the ET components and soil infiltration were
276 selected as variables for comparison. In addition, correlations were examined as scatter plots to
277 ensure that possible sensitivity not captured by the monotonic correlation coefficient was not
278 overlooked.

279 2.2.2 Method to distribute 1-D simulations spatially

280 Groundwater recharge was estimated for a model domain of 82.3 km² (Fig. 1). To distribute the
281 simulations in 1-D soil column spatially, the simulation domain was subdivided into different
282 recharge zones, similarly to e.g. Jyrkämä et al. (2002). Zonation in the model was based on two
283 variables: LAI and unsaturated zone thickness (UZT). The calculation of spatially distributed
284 values for LAI and UZT is presented in detail in sections 2.1.1 and 2.1.4. Both variables were
285 presented as a grid maps with 20m x 20m cell size with a floating point number assigned to
286 each cell, resulting in a total of 205 708 cells for the model domain. The small model cell size
287 was selected to ensure full exploitation of the forest inventory plots in LAI determination. The
288 spatially distributed data were then divided into 15 classes for LAI and 30 classes for UZT. The
289 classes are primarily equal intervals, which was convenient in the subsequent data processing,
290 but in addition the frequency distributions of LAI and UZT cell values were used to assign
291 narrower classes for parameter ranges with many values (see histograms in Figs. 3 and 4). Class
292 interval for LAI was 0.2 units up to a value of 2 (class 1: LAI = 0-0.2, etc.) and 0.3 to the
293 maximum LAI value of 3.5. Class interval for UZT was 1 m to 10 m depth and 2 m to the final
294 depth of 51 m. Finally, the classified LAI and UZT data were combined to a raster map with
295 20m x 20m cell size, producing 449 different zones with unique combinations of LAI and UZT
296 values. Spatial coupling was done with the ArcGIS software (ESRI, 2011).

297 Variation in the LAI and UZD parameters were used to allocate the 1-D soil profile simulations
 298 spatially to the study site. LAI class in model cell specified a subset of the 400 1-D simulations
 299 that were applicable for a given cell. UZT class for each cell (Fig. 2) specified the depth in the
 300 simulated 51 m soil profile where the water flux output was extracted. Using this approach each
 301 unique recharge zone (a combination of UZT and LAI class) had on average 27 water flow time
 302 series (number of total model runs [400] divided by number of LAI cell classes [15]) produced
 303 by different random combinations of parameters (Table 2). Equation (3) was used to propagate
 304 the variability in the 27 time series into the final areal recharge.

$$305 \quad R_{i,j} = \frac{\sum_{l=1}^{449} n(l) * R_{s_i,rand(1:k)} * A_c}{A_{tot}} \quad (3)$$

306 where $R_{i,j}$ is the final sample of areal recharge [mm day^{-1}], i is the index for simulation time
 307 step (= 1:14975), j is the index for sample for a given time step (1:150), l is the index for unique
 308 recharge zone, $n(l)$ is the number of cells in a given recharge zone, R_s is the recharge sample
 309 [mm/day] for a given recharge zone at time step l , k is the number of time series for a given
 310 recharge zone, A_c is the surface area of a model raster cell ($=20 \text{ m} * 20 \text{ m} = 400 \text{ m}^2$), and A_{tot}
 311 is the surface area of the total recharge area.

312 The resulting R matrix has 150 time series for areal recharge produced by simulations with
 313 different parameter realizations. The variability between the time series provides an indication
 314 of how much the simulated recharge varies due to different model parameter values. The
 315 method allows computationally efficient recharge simulations, because the different recharge
 316 zones do not all have to be simulated separately.

317 The simulation approach assumes that: (1) over the long-term, the water table remains at a
 318 constant level, i.e. the unsaturated thickness for each model cells stays the same. Monitoring
 319 data from 11 boreholes and seven lakes with more than 5 years of observation history shows
 320 level variability of 1 – 1.5 m, with depressions and recoveries of the water table. This variability
 321 is within the accuracy of water table estimation by interpolation. (2) the capillary fringe in the
 322 sandy soil is thin enough not to affect the water flow before arriving at the ‘imaginary’ water
 323 table at the center of each soil class. (3) only vertical flow takes place in the unsaturated soil
 324 matrix, a typical assumption in recharge estimation techniques (Dripps and Bradbury, 2010,
 325 Jyrkama et al., 2002, Scanlon et al., 2002a). (4) surface runoff is negligible primarily due to the
 326 permeable soil type (as noted by Keese et al., 2005), and also due to lichen cover inhibiting
 327 runoff by increasing surface roughness (Rodríguez-Caballero et al., 2012). The maximum

328 observed daily rainfall for the area has been 57.4 mm. Further assuming that rain for the day
329 fell only during one hour, it would equal to $1.59 \cdot 10^{-5} \text{ m s}^{-1}$ input rate of water, which is close
330 to the lower range of saturated hydraulic conductivity at the study site ($1.99 \cdot 10^{-5} \text{ m s}^{-1}$).
331 Therefore rainstorms at the site very rarely exceed the theoretical infiltration capacity. As a
332 field verification, surface runoff has not been observed during field visits and the area lacks
333 intermittent or ephemeral stream networks.

334 2.2.3 Estimation of evapotranspiration

335 Four different evaporation processes were considered in this study (Fig. 5); soil evaporation
336 (evaporation from the topmost soil layer, i.e. the lichen matrix), snow evaporation (evaporation
337 from snow surface), transpiration (evaporation through the vascular system of tree canopy) and
338 lake evaporation (evaporation from free water surface). In areas with unsaturated soil zones,
339 the first three components were estimated, along with water flow simulations, using
340 CoupModel. However, as 3.6 % (2.9 km^2) of the surface area of the study site consists of lakes
341 (Fig. 1), lake evaporation from free water surfaces was calculated independently from the
342 CoupModel simulations.

343 Transpiration from the Scots pine canopy ($L_v E_{tp}$) was calculated using Penman-Monteith (P-
344 M) combination (Appendix 1, Eq. 1). Whenever possible, all the parameters relating to the P-
345 M equation were estimated based on data, namely LAI of the canopy. Surface resistance and
346 saturation vapor pressure difference are the main factors controlling conifer forest
347 evapotranspiration, while the aerodynamic resistance is of less importance (Lindroth, 1985,
348 Ohta et al., 2001). In the calculation of aerodynamic resistance with the P-M equation,
349 roughness length is related to LAI and canopy height, according to Shaw and Pereira (1982).
350 Other parameters governing the aerodynamic resistance, except for LAI, were treated as
351 constant. The surface resistance of the pine canopy was estimated with the Lohammar equation
352 (see e.g. Lindroth, 1985), accounting for effects of solar radiation and air moisture deficit in
353 tree canopy gas exchange. Because LAI values have a strong influence in the surface resistance
354 Lohammar equation, the other parameters governing the surface resistance were excluded from
355 the Monte Carlo runs. Distribution of root biomass with respect to depth from the soil surface
356 was presented with an exponential function, because most Scots pine roots are concentrated in
357 the shallow soil zone. A typical root depth value of 1 m was used for the entire canopy
358 (Kalliokoski, 2011, Kelliher et al., 1998, Vincke and Thiry, 2008). Soil and snow evaporation
359 were calculated using an empirical approach (Appendix 1, Eq. 4) based on the P-M equation,

360 as described in detail in Jansson and Karlberg (2004). Soil evaporation is calculated for the
361 snow-free fraction of the soil surface, and the snow evaporation is solved separately as a part
362 of snow pack water balance.

363 In areas where the water table is close to the ground surface, the water table can provide an
364 additional source of water for evapotranspiration (Smerdon et al., 2008). To take into account
365 the decreased recharge for areas with near surface water tables, the recharge for cells with an
366 unsaturated zone of <1 m (8.3% of the study site, 6.8 km²) was estimated with a water balance
367 approach. We assumed that for areas with a shallow water table, soil water content was not a
368 limiting factor for transpiration. Therefore an additional water source for transpiration was
369 considered by making the transpiration rate equal to simulated potential transpiration (T) during
370 times when the actual transpiration was simulated (T > 0.05 mm). Increasing effect of the water
371 table located at 1 m depth on soil evaporation was tested with simulations and found to be 5-
372 10% higher with than without a water table. Therefore a 7% addition was made to the simulated
373 actual soil evaporation for cells with a shallow water table. Daily recharge (R_{1m} , L T⁻¹) for cells
374 with unsaturated thickness below 1 m was estimated as:

$$375 \quad R_{1m} = I - T_{adj} - ES_{adj} \quad (4)$$

376 where I is infiltration water arriving to lake/soil surface, including both meltwater from the
377 snowpack and precipitation [L T⁻¹], T_{adj} [mm d⁻¹] is adjusted transpiration, and ES_{adj} [mm d⁻¹]
378 is adjusted soil evaporation. Kettle hole lakes in esker aquifers often lack surface water inlets
379 and outlets and are therefore an integral part of the groundwater system (Ala-aho et al., 2013,
380 Winter et al., 1998), so we considered these lakes as contributors to total groundwater recharge.
381 In other words, rainfall per lake surface area is treated equally as addition to the aquifer water
382 storage as groundwater recharge. As a difference, lake water table is subjected to evaporation
383 unlike the groundwater table. Lake evaporation (E_{lake}) was estimated with the mass transfer
384 approach (see e.g. Dingman, 2008) according to Eq. (7) in Appendix 1. The mass transfer
385 method was selected because of its simplicity, daily output resolution, low data requirement,
386 and physically-based approach. However various calculation methods could easily be used in
387 the modelling framework, depending on the data availability (see e.g. Rosenberry et al., 2007).
388 If lake percentage in the area of interest is high, more sophisticated methods may be required
389 to better represent the system. For the Rokua site the bias introduced by a simplistic approach
390 was considered minor.

391 **2.3 Model validation**

392 Model performance was tested by comparing the simulated recharge values with two
393 independent recharge estimates in local and regional scale; the water table fluctuation (WTF)
394 method and base flow estimation, respectively. The WTF method is routinely used to estimate
395 groundwater recharge because of its simplicity and ease of use. It assumes that any rise in water
396 level in an unconfined aquifer is caused by recharge arriving at the water table. For a detailed
397 description of the method and its limitations, see e.g. Healy and Cook (2002). The recharge
398 amount (R , $L T^{-1}$) is calculated based on the water level prior to and after the recharge event
399 and the specific yield of the soil:

$$400 \quad R = S_y \frac{\Delta h}{\Delta t} \quad (5)$$

401 where S_y is the specific yield, h is the water table height [L], and t is the time of water table rise
402 [T].

403 The WTF method requires groundwater level data with adequate resolution for both time and
404 water level, to identify periods of rising and falling water table. Water table was monitored
405 using pressure-based dataloggers (Solinst Levellogger Gold) recording with hourly interval
406 from six water table wells with average unsaturated zone thicknesses of 1.2, 1.6, 5.0, 8.0, 9.3,
407 and 14.7 m (Fig. 1). Wells where the water table was <2 m from the ground surface responded
408 to major precipitation events. In the deeper wells, only the recharge from snowmelt was seen
409 as water table rise. Estimates of the soil specific yield are required for the calculations (Eq. 5),
410 but no soil samples were available from the wells used in water table monitoring. Drilling
411 records for these wells reported fine and medium sand, which was consistent with the particle
412 size distribution for other wells in the area. Therefore an estimated value of 0.20-0.25 for the
413 specific yield of all wells was used, according to typical values for fine and medium sand
414 (Johnson, 1967).

415 The recharge estimated with the WTF method was compared with the simulated recharge
416 during the recorded water level rise in the well. For each well, the cumulative sum of simulated
417 water flow was extracted from soil profile depth corresponding to well water table depth. As
418 an example, the simulated recharge in well ROK1 (unsaturated thickness on average 14.7 m)
419 was extracted from soil class 12, corresponding to recharge for unsaturated thickness of 14-16
420 m. All 400 model runs were used, providing 400 estimates for recharge for each time period of
421 recorded water level rise.

422 A regional estimate of groundwater recharge was estimated as baseflow of streams originating
423 at the groundwater discharge area. Because the Rokua esker aquifer acts as a regional water
424 divide, stream flow was monitored around the esker, in total of 18 locations (Fig. 1). The flows
425 were measured total of 8 times between 6 July 2009 and 3 August 2010 (see Rossi et al., 2014).
426 The lowest total outflow during 9-10 February 2010 was recorded after three months of snow
427 cover period, when water contribution to streams from surface runoff was minimal. The
428 minimum outflow was considered as baseflow from the aquifer reflecting long term
429 groundwater recharge in the area.

430

431 **3 Results**

432 **3.1 Model validation with the WTF and baseflow methods**

433 Model validation showed that the modeling approach could reasonably reproduce (1) the main
434 groundwater recharge events when compared to the WTF method (Fig. 6) and (2) the regional
435 level of recharge compared to stream baseflow. The WTF method agreed well with the
436 simulated values, with overlapping estimates between the methods for all but two recharge
437 events. Also the median value of simulations was close to WTF method, with some bias to
438 higher estimates from the simulations. The discrepancy can be due to very different assumptions
439 behind the methods and uncertainty in local parameterization; in the WTF method for the
440 specific yield (S_y) and for simulations mainly the hydraulic conductivity which dictates the
441 simulated timing of recharge. Uncertainty in the S_y estimate is acknowledged by showing S_y a
442 range rather than a single value (Fig. 6), but still S_y is not truly known for the location of
443 observation boreholes. Simplifying assumptions and subjective interpretation of both timing
444 and height of water table rise create additional inaccuracies in the WTF estimate.

445 Independent regional estimate of recharge, stream baseflow, was $70\,500\text{ m}^3\text{ s}^{-1}$, or 312.7 mm
446 a^{-1} when related to the recharge area. The order of magnitude agreed with long term simulated
447 average of 362.8 mm a^{-1} . Typical error in individual stream flow measurements is within 3-6 %
448 of the measured value (Sauer and Meyer, 1992), which brings minor uncertainty in the baseflow
449 value. The smaller value for stream baseflow compared to simulated long term average recharge
450 can be explained with conceptual understanding of site hydrogeology (Ala-aho et al., 2015,
451 Ala-aho et al., 2013, Rossi et al., 2012, Rossi et al., 2014). Part of the recharged groundwater
452 does not discharge to the small streams whose baseflow was measured, but flows underneath

453 the stream catchments and seeps out to regional surface bodies (Lake Oulujärvi and River
454 Oulujoki) further away from the recharge area (Fig. 2). Fully integrated surface-subsurface
455 hydrological modeling study of the same site presented in Ala-aho et al. (2015) simulated an
456 outflow of 79 mm a⁻¹ to regional surface water bodies.

457 **3.2 Temporal variations in groundwater recharge**

458 When recharge simulation time series were summarized to annual values (1 Oct-30 Sept),
459 recharge rates co-varied with annual infiltration with linear correlation coefficient of 0.89
460 (Fig. 7) as expected based on previous work in humid climate and sandy soils (Keese et al.,
461 2005, Lemmelä, 1990). Both annual recharge and infiltration displayed an increasing trend. The
462 plot also showed the level of uncertainty in annual recharge values introduced by differences
463 in model parameterization (black area). The difference between minimum and maximum value
464 for simulated annual recharge was on average 23.0 mm. Thus the variability in recharge
465 estimates was 6.3 % of mean annual recharge 362.8 mm.

466 According to the simulations, the *effective rainfall*, i.e. the percentage of corrected rainfall
467 resulting in groundwater recharge annually, was on average 59.3%. This is in agreement with
468 previous studies on unconfined esker aquifers at northerly latitudes, in which the proportion of
469 annual precipitation percolating to recharge is reported to be 50-70% (71% by Zaitsoff (1984),
470 54% by Lemmelä and Tattari (1986) and 56% by Lemmelä (1990)). The percentage of effective
471 rainfall varied considerably, by almost 30 %-units, between different hydrological years, from
472 44.8% in some years up to 73.1% in others.

473 **3.3 Influence of LAI on spatial variation of groundwater recharge**

474 The spatial distribution of groundwater recharge was mostly due to variations in LAI, but also
475 influenced by distance to water table, and distribution of lakes (Fig. 8). Higher evaporation rates
476 from lakes led to lower recharge in lakes (see red spots in Fig. 8). Similarly, high LAI led to
477 high ET and resulted in low recharge in plots with high LAI. Other areas of low recharge,
478 although not as obvious at the larger spatial scales shown in Fig. 8, were cells with a shallow
479 water table (section 2.2.2). The effect of high ET at locations with a shallow water table can
480 best be seen in south-east parts of the aquifer.

481 Kendall correlation analysis of simulation parameters and annual average model outputs
482 identified LAI as the most important parameter controlling evapotranspiration and infiltration

483 (Table 3). Parameters related to soil hydraulics and evaporation showed some sensitivity to
484 simulation results, while the parameters for lichen vegetation were only slightly sensitive or
485 insensitive to simulation output variables. The LAI parameter governed the level of evaporation
486 for different ET components (Fig. 9). Evaporation from soil (and snow) compensated for mean
487 annual ET for LAI values up to around 1.0, after which total ET increased as a function of LAI.
488 The scenarios for low (0 ... 0.2) and high (3.2 ... 3.5) LAI changed the groundwater recharge
489 rates compared to the current LAI distribution (in Fig. 7). In the high LAI scenario the annual
490 recharge was on average 101.7 mm lower than in the low LAI scenario. These results suggest
491 that management of the Scots pine canopy has a significant control on the total recharge rates
492 in unconfined esker aquifers.

493 Average land surface ET components remained relatively constant between years, but the
494 simulated ET displayed a wide spread between simulations (Fig. 10). Estimated annual
495 evapotranspiration (mean 237.6 mm) was somewhat lower than previous regional estimates of
496 total ET (300 mm; (Mustonen, 1986)). Lake evaporation rates were generally higher than
497 evapotranspiration from the land surface (420.0 mm). The variation in simulated lake
498 evaporation was considerably lower than that in ET, as a different approach was used to account
499 for uncertainty in the simulations. Transpiration showed greater variation between simulations
500 than soil evaporation and total land surface ET. On average, transpiration also comprised a
501 slightly larger share of total evaporation than soil evaporation. Simulated snow evaporation was
502 a small, yet not insignificant, component in the total ET.

503 **4 Discussion**

504 The method used here to estimate LAI from forestry inventories introduces a new approach for
505 incorporating large spatial coverage of detailed conifer canopy data into groundwater recharge
506 estimations. LAI values reported for conifer forests in Nordic conditions similar to the study
507 site are in the range 1-3, depending on canopy density and other attributes (Koivusalo et al.,
508 2008, Rautiainen et al., 2012, Vincke and Thiry, 2008, Wang et al., 2004). The LAI values
509 obtained for the study site (mean 1.25) were at the lower end of this range. Furthermore, the
510 data showed a bimodal distribution, with many model cells with low LAI (< 0.4) lowering the
511 mean LAI. The low LAI values were expected because of active logging and clearcutting
512 activities in the study area. Although the equations to estimate LAI are empirical in nature and
513 based on simplified assumptions, the method can outline spatial differences in canopy structure.
514 Wider use of this method in Finland is practically possible, as active forestry operations in

515 Finland have yielded an extensive database on canopy coverage, which could be used in
516 groundwater management. However, the LAI estimation method could be further validated with
517 field measurements or Lidar techniques (Chasmer et al., 2012, Riaño et al., 2004).

518 Plant cover, represented as LAI, proved to be the most important model parameter important
519 parameter controlling total ET, and thereby the amount of groundwater recharge (Table 3, Fig.
520 9). The LAI parameter was included in the equations controlling both transpiration and soil
521 evaporation, and therefore the sensitivity of the parameter is not surprising. While soil
522 evaporation partly compensated for the lower transpiration with low LAI values, the total
523 annual ET values progressively increased as a function of LAI (Fig. 9). Interestingly, the
524 simulations suggested that ET remains constant at constant level in the LAI range 0-1,
525 potentially due to the sparse canopy changing the aerodynamic resistance and partitioning of
526 radiation limiting soil evaporation, while still not contributing much to transpiration in total ET.
527 This implies that the maximum groundwater recharge for boreal Scots pine remains rather
528 constant up to a threshold LAI value of around 1. This knowledge can be used when co-
529 managing forest and groundwater resources in order to optimize both.

530 Importance of LAI has been reported in earlier studies estimating groundwater recharge
531 (Dripps, 2012, Keese et al., 2005, Sophocleous, 2000), but here the vegetation was represented
532 with more spatially detailed patterns and a field data-based approach for LAI. According to
533 previous studies, average ET from boreal conifer forests is around 2 mm d^{-1} during the growing
534 season (Kelliher et al., 1998), which is similar to our average value of 1.6 mm d^{-1} for the period
535 1 May-31 Oct. Some earlier studies have claimed that the influence of LAI on total ET rates
536 from boreal conifer canopies is minor (Kelliher et al., 1993, Ohta et al., 2001, Vesala et al.,
537 2005), but our simulation results indicate that higher LAI values lead to higher total ET values.
538 The simulations showed that variable intensity of forestry, from low canopy coverage (LAI =
539 0-0.2) to dense coverage (LAI = 3.2-3.5) resulted in a difference of over 100 mm in annual
540 recharge (Fig. 7). It can be argued that the scenarios are unrealistic, because high LAI values,
541 covering the whole study site, may not be achieved even with a complete absence of forestry
542 operations. Nevertheless, the result demonstrates a substantial impact of forestry operations on
543 esker aquifer groundwater resources. The lichen layer covering the soil surface was explicitly
544 accounted for in the simulation set-up, which to our knowledge is a novel modification. Kelliher
545 et al. (1998) concluded that precipitation intercepted by lichen was an important source of
546 understorey evaporation, especially directly after rain events. In addition, Bello and Arama

547 (1989) reported that lichen could intercept light rain showers completely and that only intense
548 rain events caused drainage from lichen canopy to mineral soil. While the lichen layer might
549 have an increasing effect on soil evaporation through ‘interception storage’, Fitzjarrald and
550 Moore (1992) suggest that a lichen cover may in fact have an insulating influence on heat and
551 vapor exchange between soil and atmosphere, therefore impeding evaporation from the mineral
552 soil. In the present study, the lichen layer appeared to have minor influence on total evaporation,
553 soil evaporation and infiltration, as these variables showed only little sensitivity to lichen B&C
554 parameters (Table 3). However, the approach to represent lichen with B&C model needs to
555 better examined, as water retention capacity of lichen layer was treated equal to porosity, which
556 is not strictly coherent with the Brooks and Corey (B&C) model. Nevertheless, the used
557 approach successfully produced an additional interception storage of water in the correct range
558 (generally 3-7 mm depending on random parameterization, data not shown). The performed
559 laboratory measurement of lichen water retention should be supplemented with detailed
560 analysis of lichen pressure-saturation curve and hydraulic conductivity to clarify the role of
561 lichen in soil evaporation, and thereby groundwater recharge.

562 Stochastic variation of selected model parameters illustrated the uncertainties relating to
563 numerical recharge estimation using the Richards equation in one dimension. The capability
564 and robustness of the Richards equation to reproduce soil water content and water fluxes have
565 been demonstrated extensively in various studies (Assefa and Woodbury, 2013, Scanlon et al.,
566 2002b, Stähli et al., 1999, Wierenga et al., 1991). Therefore we considered that model
567 calibration and validation with point observations of variables such as soil volumetric water
568 content or soil temperature would not provide novel insights into water flow in unsaturated
569 soils. Instead, we incorporated the parameter uncertainty ranges, usually used in model
570 calibration, to the final recharge simulation output. An important outcome was that the
571 uncertainty in the model output caused by different model parameterizations was small in
572 comparison with the interannual variation in recharge. The error caused by uncertainty in the
573 model assumptions or driving climate data was not addressed in this study.

574 The sensitivity analysis focused on total cumulative values of fluxes and did not address the
575 temporal variations in the variables. Soil hydraulic parameters mainly influenced the timing of
576 recharge through residence time in the soil, not so much the total amount. Therefore the soil
577 hydraulic parameters showed only minor sensitivity, perhaps misleadingly. It should be noted
578 that vertical heterogeneity in the soil profile hydraulic parameters can reduce the total recharge

579 rates (Keese et al., 2005). However, vertical heterogeneities were ignored in this study not only
580 to simplify the model, but also because the drilling logs showed only little variation in the area.
581 Work of Wierenga et al. (1991) supports the simplification by showing that excluding moderate
582 vertical heterogeneities does not significantly affect the performance of water flow simulations
583 with the Richards equation.

584 Simulations acknowledged shallow water table contribution to evapotranspiration in an
585 indirect, conceptual approach. Including a water table fixed at different depths in the soil profile
586 would have been possible in the CoupModel setup. Influence of water table fixed at 2 m depth
587 was tested and found to increase ET 3.5% for LAI values of 3, but for LAI values of 0.5 and
588 1.5 the increase in ET was only trivial. We expect only minor increase in ET with deeper water
589 table configuration (with the given soil type), and therefore argue that excluding water table
590 results in only minimal overestimation of total recharge at the study site. It should be noted that
591 upward water fluxes were not excluded from the water flow time series and negative fluxes
592 were considered as “negative recharge” at any depth. The simplification is made that water
593 available for upward fluxes comes only from the soil moisture storage, not from the water table.

594 According to the simulations, the percentage of precipitation forming groundwater recharge
595 varied considerably between years, as also reported in previous studies on transient recharge
596 (Assefa and Woodbury, 2013, Dripps and Bradbury, 2010). Even though annual recharge was
597 correlated with annual precipitation, and therefore years with high precipitation resulted in
598 higher absolute recharge (Fig. 7), the percentage of effective rainfall did not increase as a
599 function of annual sum of precipitation. This is somewhat surprising, because the rather
600 constant evaporation potential between years (Fig. 10) and high soil hydraulic conductivity
601 could be expected to result in a higher percentage of rainfall reaching the water table in rainy
602 years. Some studies (Dripps and Bradbury, 2010, Okkonen and Kløve, 2010) have suggested
603 that when the main annual water input arrives as snowmelt during the low evaporation season,
604 it is likely to result in higher percentage recharge than in a year with little snow storage and
605 precipitation distributed evenly throughout summer and autumn, which may contribute to the
606 variability in the effective rainfall coefficient. However, when the maximum annual SWE value
607 was used as a proxy for annual snow storage, there was no evidence of snow amount explaining
608 the interannual variability in the recharge coefficient. Other factors contributing to recharge
609 coefficient variability may be related to soil moisture conditions prior to snowfall, or the
610 intensity of summer precipitation events (Smerdon et al., 2008, Stähli et al., 1999).

611 The above-mentioned reasons make the concept of effective rainfall, which is currently
612 routinely used to estimate groundwater recharge for groundwater management in e.g. Finland
613 (Britschgi et al., 2009), susceptible to over- or under-estimation of actual annual recharge. This
614 applies especially for aquifers with a thick unsaturated zone, where rainy years produce higher
615 average recharge with some delay and for a longer duration (Zhou, 2009).

616

617 **5 Conclusions**

618 A physically-based approach to simulate groundwater recharge for sandy unconfined aquifers
619 in cold climates was developed. The method accounts for the influence of vegetation,
620 unsaturated zone thickness, presence of lakes, and uncertainty in simulation parameters in the
621 recharge estimate. It is capable of producing spatially and temporally distributed groundwater
622 recharge values with uncertainty margins, which are generally lacking in recharge estimates,
623 despite understanding of uncertainty related to recharge estimates being potentially crucial for
624 groundwater resource management. However, the parameter uncertainty defined for the study
625 area was of minor significance compared with interannual variations in the recharge rates
626 introduced by climate variations.

627 The simulations showed that Scots pine canopy, parameterized as leaf area index (LAI), was
628 important in controlling the total amount of groundwater recharge. Forestry inventory databases
629 were used to estimate and spatially allocate the LAI and the results showed that such inventories
630 could be better utilized in groundwater resource management. Forest cuttings were
631 demonstrated to increase groundwater recharge significantly. A sensitivity analysis on the
632 parameters used showed that soil evaporation could compensate for low LAI-related
633 transpiration up to a LAI value of approximately 1, which may be important in finding the
634 optimal level for forest management in groundwater resource areas. The concept of effective
635 rainfall gave inconsistent estimates of recharge in annual timescales, showing the importance
636 of using physically-based recharge estimation methods for sustainable groundwater recharge
637 management.

638

639

640

641

642 **Author contribution**

643 P. Ala-aho and P.M Rossi collected and analyzed the field data. P. Ala-aho designed the
644 simulation set-up, performed the simulations and interpreted the results. P. Ala-aho prepared
645 the manuscript with contributions from all co-authors.

646

647 **Acknowledgements**

648 This study was made possible by the funding from EU 7th Framework programme GENESIS
649 (Contract Number 226536), Academy of Finland AKVA research program, the Renlund
650 Foundation, VALUE doctoral school and Maa- ja vesitekniikantuki ry. We would like to
651 express our gratitude to Geological survey of Finland, Finnish Forest Administration
652 (Metsähallitus) and Finnish Forest Centre (Metsäkeskus), Finnish meteorological institute,
653 Finnish environmental administration and National land survey of Finland for providing
654 datasets and expert knowledge that made this study possible in its current extent. To reproduce
655 the research in the paper, data from above mentioned agencies can be made available for
656 purchase on request from the corresponding agency, other data can be provided by the
657 corresponding author upon request. We thank Per-Erik Jansson for his assistance with the
658 CoupModel and Jarkko Okkonen (GTK) and two anonymous reviewers for their critical
659 comments that improved the manuscript.

660

661

662

663

664

665

666

667

668

669

670

671 **References**

- 672 Aartolahti, T.: Morphology, vegetation and development of Rokuanvaara, an esker and dune
673 complex in Finland, *Societas geographica Fenniae*, Helsinki, 1973.
- 674 Ala-aho, P., Rossi, P. M. and Kløve, B.: Interaction of esker groundwater with headwater
675 lakes and streams, *J. Hydrol.*, 500, 144-156, doi:10.1016/j.jhydrol.2013.07.014, 2013.
- 676 Ala-aho, P., Rossi, P. M., Isokangas, E. and Kløve, B.: Fully integrated surface–subsurface
677 flow modelling of groundwater–lake interaction in an esker aquifer: Model verification with
678 stable isotopes and airborne thermal imaging, *J. Hydrol.*, 522, 391-406,
679 doi:10.1016/j.jhydrol.2014.12.054, 2015.
- 680 Allen, R., Pereira, L., Raes, D. and Smith, M.: Crop evapotranspiration - Guidelines for
681 computing crop water requirements, Food and Agriculture Organization of the United
682 Nations, Rome, 1998.
- 683 Assefa, K. A. and Woodbury, A. D.: Transient, spatially- varied groundwater recharge
684 modelling, *Water Resour. Res.*, 49, 1-14, doi:10.1002/wrcr.20332, 2013.
- 685 Banerjee, I., McDonald, B.C.: Nature of esker sedimentation, in: *Glaciofluvial and*
686 *Glaciolacustrine Sedimentation*, edited by: Jopling, A. V. and McDonald, B. C., *Soc. Econ.*
687 *Paleontol. Mineral.*, Tulsa, U.S.A, 132-155, 1975
- 688 Bello, R. and Arama, A.: Rainfall interception in lichen canopies, *Climatol. Bull*, 23, 74-78,
689 1989.
- 690 Bent, G. C.: Effects of forest-management activities on runoff components and ground-water
691 recharge to Quabbin Reservoir, central Massachusetts, *For. Ecol. Manage.*, 143, 115-129,
692 2001.
- 693 Blum, O. B.: Water relations, in: *The lichens*, Ahmadjian, V. and Hale, M. E. (Eds.),
694 Academic Press Inc., USA, 381-397, 1973.
- 695 Bolduc, A., Paradis, S. J., Riverin, M., Lefebvre, R. and Michaud, Y.: A 3D esker geomodel
696 for groundwater research: the case of the Saint-Mathieu–Berry esker, Abitibi, Quebec,
697 Canada, in: *Three-Dimensional Geologic Mapping for Groundwater Applications: workshop*
698 *extended abstracts*, 17-20, Salt Lake City, Utah, 15 Oct, 2005.
- 699 Britschgi, R., Antikainen, M., Ekholm-Peltonen, M., Hyvärinen, V., Nylander, E., Siiro, P.
700 and Suomela, T.: Mapping and classification of groundwater areas, *The Finnish Environment*
701 *Institute*, Sastamala, Finland, 75 pp., 2009.
- 702 Chasmer, L., Pertrone, R., Brown, S., Hopkinson, C., Mendoza, C., Diiwu, J., Quinton, W.
703 and Devito, K.: Sensitivity of modelled evapotranspiration to canopy characteristics within
704 the Western Boreal Plain, Alberta, in: *Remote Sensing and Hydrology, Proceedings of a*
705 *Symposium at Jackson Hole*, 337-341, Wyoming, USA, 27-30 September 2010, 2012.

- 706 Croteau, A., Nastev, M. and Lefebvre, R.: Groundwater recharge assessment in the
707 Chateauguay River watershed, *Canadian Water Resources Journal*, 35, 451-468, 2010.
- 708 Dingman, S. L.: *Physical hydrology*, Waveland Press Inc, Long Grove, IL, 2008.
- 709 Dripps, W.: *An Integrated Field Assessment of Groundwater Recharge*, *Open Hydrology*
710 *Journal*, 6, 15-22, 2012.
- 711 Dripps, W. and Bradbury, K.: The spatial and temporal variability of groundwater recharge in
712 a forested basin in northern Wisconsin, *Hydrol. Process.*, 24, 383-392, doi:10.1002/hyp.7497,
713 2010.
- 714 Dripps, W. and Bradbury, K.: A simple daily soil–water balance model for estimating the
715 spatial and temporal distribution of groundwater recharge in temperate humid areas,
716 *Hydrogeol. J.*, 15, 433-444, doi:10.1007/s10040-007-0160-6, 2007.
- 717 EC: Directive 2006/118/EC of the European Parliament and of the Council on the protection
718 of groundwater against pollution and deterioration, Bryssels, Belgium, 2006.
- 719 ESRI: *ArcGIS Desktop: Release 10*, Environmental Systems research institute, Redlands,
720 Texas, 2011.
- 721 Finnish environmental administration: Oiva – the environmental and geographical
722 information service, Helsinki, Finland, Observation station number 5903320, Data extracted
723 27 June 2013, 2013.
- 724 Finnish environmental administration: Oiva – the environmental and geographical
725 information service, Helsinki, Finland, Observation station number 1592101, Data extracted
726 11 Feb 2011, 2011.
- 727 Fitzjarrald, D. R. and Moore, K. E.: Turbulent transports over tundra, *J. Geophys. Res.*, 97,
728 16717-16729, 1992.
- 729 Healy, R. W. and Cook, P. G.: Using groundwater levels to estimate recharge, *Hydrogeol. J.*,
730 10, 91-109, 2002.
- 731 Hunt, R. J., Prudic, D. E., Walker, J. F. and Anderson, M. P.: Importance of unsaturated zone
732 flow for simulating recharge in a humid climate, *Ground Water*, 46, 551-560, 2008.
- 733 Jansson, P. and Karlberg, L.: *Coupled heat and mass transfer model for soil-plant-atmosphere*
734 *systems*, Royal Institute of Technology, Dept of Civil and Environmental Engineering,
735 Stockholm, 435 pp., 2004.
- 736 Johnson, A. I.: *Specific yield: compilation of specific yields for various materials*, US
737 Government Printing Office, Washington, 1967.
- 738 Jyrkama, M. I. and Sykes, J. F.: The impact of climate change on spatially varying
739 groundwater recharge in the grand river watershed (Ontario), *J. Hydrol.*, 338, 237-250, 2007.

- 740 Jyrkama, M. I., Sykes, J. F. and Normani, S. D.: Recharge estimation for transient ground
741 water modeling, *Ground Water*, 40, 638-648, 2002.
- 742 Kalliokoski, T.: Root system traits of Norway spruce, Scots pine, and silver birch in mixed
743 boreal forests: an analysis of root architecture, morphology, and anatomy, Ph.D. thesis,
744 Department of Forest Sciences, Faculty of Agriculture and Forestry, University of Helsinki,
745 2011.
- 746 Karjalainen, T., Rossi, P., Ala-aho, P., Eskelinen, R., Reinikainen, K., Kløve, B., Pulido-
747 Velazquez, M. and Yang, H.: A decision analysis framework for stakeholder involvement and
748 learning in groundwater management, *Hydrol. Earth Syst. Sci.* 17, 5141-5153,
749 doi:10.5194/hess-17-1-2013, 2013.
- 750 Keese, K. E., Scanlon, B. R. and Reedy, R. C.: Assessing controls on diffuse groundwater
751 recharge using unsaturated flow modeling, *Water Resour. Res.*, 41, W06010,
752 doi:10.1029/2004WR003841, 2005.
- 753 Kelliher, F. M., Leuning, R. and Schulze, E. D.: Evaporation and canopy characteristics of
754 coniferous forests and grasslands, *Oecologia*, 95, 153-163, 1993.
- 755 Kelliher, F. M., Lloyd, J., Arneth, A., Byers, J. N., McSeveny, T. M., Milukova, I., Grigoriev,
756 S., Panfyorov, M., Sogatchev, A., Varlargin, A., Ziegler, W., Bauer, G. and Schulze, E. -:
757 Evaporation from a central Siberian pine forest, *J. Hydrol.*, 205, 279-296,
758 doi:10.1016/S0022-1694(98)00082-1, 1998.
- 759 Kløve, B., Ala-aho, P., Bertrand, G., Boukalova, Z., Ertürk, A., Goldscheider, N., Ilmonen, J.,
760 Karakaya, N., Kupfersberger, H., Kværner, J., Lundberg, A., Mileusnić, M., Moszczynska,
761 A., Muotka, T., Preda, E., Rossi, P., Siergieiev, D., Šimek, J., Wachniew, P., Angheluta, V.
762 and Widerlund, A.: Groundwater dependent ecosystems. Part I: Hydroecological status and
763 trends, *Environ. Sci. & Policy*, 14, 770-781, doi:10.1016/j.envsci.2011.04.002, 2011.
- 764 Koivusalo, H., Ahti, E., Laurén, A., Kokkonen, T., Karvonen, T., Nevalainen, R. and Finér,
765 L.: Impacts of ditch cleaning on hydrological processes in a drained peatland forest,
766 *Hydrol. Earth Syst. Sci.*, 12, 1211-1227, 2008.
- 767 Koundouri, P., Kougea, E., Stithou, M., Ala-Aho, P., Eskelinen, R., Karjalainen, T. P., Klove,
768 B., Pulido-Velazquez, M., Reinikainen, K. and Rossi, P. M.: The value of scientific
769 information on climate change: a choice experiment on Rokua esker, Finland, *Journal of*
770 *Environmental Economics and Policy*, 1, 85-102, 2012.
- 771 Kumpula, J., Colpaert, A. and Nieminen, M.: Condition, potential recovery rate, and
772 productivity of lichen (*Cladonia* spp.) ranges in the Finnish reindeer management area, *Arctic*,
773 53, 152-160, 2000.
- 774 Kurki, V., Lipponen, A. and Katko, T.: Managed aquifer recharge in community water
775 supply: the Finnish experience and some international comparisons, *Water Int.*, 38, 774-789,
776 2013.

- 777 Lagergren, F., Lankreijer, H., Kučera, J., Cienciala, E., Mölder, M. and Lindroth, A.:
778 Thinning effects on pine-spruce forest transpiration in central Sweden, *For. Ecol. Manage.*,
779 255, 2312-2323, 2008.
- 780 Larson, D. W.: Lichen water relations under drying conditions, *New Phytol.*, 82, 713-731,
781 doi:10.1111/j.1469-8137.1979.tb01666.x, 1979.
- 782 Lemmelä, R. and Tattari, S.: Infiltration and variation of soil moisture in a sandy aquifer,
783 *Geophysica*, 22, 59-70, 1986.
- 784 Lemmelä, R.: Water balance of sandy aquifer at Hyrylä in southern Finland, Ph.D. thesis,
785 University of Turku, Turku, 1990.
- 786 Lindroth, A.: Canopy Conductance of Coniferous Forests Related to Climate, *Water Resour.*
787 *Res.*, 21, 297-304, doi:10.1029/WR021i003p00297, 1985.
- 788 Mustonen, S.: *Sovellettu hydrologia, Vesiyhdistys*, Helsinki, 1986.
- 789 National Land Survey of Finland: NLS file service of open data, Laser scanning point cloud
790 (LiDAR), 2012.
- 791 Odong, J.: Evaluation of empirical formulae for determination of hydraulic conductivity
792 based on grain-size analysis, *Journal of American Science*, 3, 54-60, 2007.
- 793 Ohta, T., Hiyama, T., Tanaka, H., Kuwada, T., Maximov, T. C., Ohata, T. and Fukushima, Y.:
794 Seasonal variation in the energy and water exchanges above and below a larch forest in
795 eastern Siberia, *Hydrol. Process.*, 15, 1459-1476, doi:10.1002/hyp.219, 2001.
- 796 Okkonen, J.: Groundwater and its response to climate variability and change in cold snow
797 dominated regions in Finland: methods and estimations, Ph.D. thesis, University of Oulu,
798 Oulu, Finland, 78 pp., 2011.
- 799 Okkonen, J. and Kløve, B.: A conceptual and statistical approach for the analysis of climate
800 impact on ground water table fluctuation patterns in cold conditions, *J. Hydrol.*, 388, 1-12,
801 doi:10.1016/j.jhydrol.2010.02.015, 2010.
- 802 Okkonen, J. and Kløve, B.: A sequential modelling approach to assess groundwater-surface
803 water resources in a snow dominated region of Finland, *Journal of Hydrology*, 411, 91-107,
804 doi:10.1016/j.jhydrol.2011.09.038, 2011.
- 805 Rautiainen, M., Heiskanen, J. and Korhonen, L.: Seasonal changes in canopy leaf area index
806 and moDis vegetation products for a boreal forest site in central Finland, *Boreal*
807 *Environ. Res.*, 17, 72-84, 2012.
- 808 Repola, J., Ojansuu, R. and Kukkola, M.: Biomass functions for Scots pine, Norway spruce
809 and birch in Finland, Finnish Forest Research Institute (METLA), Helsinki, 28 pp., 2007.

- 810 Riaño, D., Valladares, F., Condés, S. and Chuvieco, E.: Estimation of leaf area index and
811 covered ground from airborne laser scanner (Lidar) in two contrasting forests, *Agric. For.*
812 *Meteorol.*, 124, 269-275, 2004.
- 813 Rodríguez-Caballero, E., Cantón, Y., Chamizo, S., Afana, A. and Solé-Benet, A.: Effects of
814 biological soil crusts on surface roughness and implications for runoff and erosion,
815 *Geomorphology*, 145, 81-89, 2012.
- 816 Rosenberry, D. O., Winter, T. C., Buso, D. C. and Likens, G. E.: Comparison of 15
817 evaporation methods applied to a small mountain lake in the northeastern USA, *Journal of*
818 *Hydrology*, 340, 149-166, 2007.
- 819 Rossi, P. M., Ala-aho, P., Ronkanen, A. and Kløve, B.: Groundwater - surface water
820 interacion between an esker aquifer and a drained fen, *J. Hydrol*, 432-433, 52-60,
821 doi:10.1016/j.jhydrol.2012.02.026, 2012.
- 822 Rossi, P. M., Ala-aho, P., Doherty, J. and Kløve, B.: Impact of peatland drainage and
823 restoration on esker groundwater resources: modeling future scenarios for management,
824 *Hydrogeol. J.*, doi:10.1007/s10040-014-1127-z, 2014.
- 825 Rothacher, J.: Increases in water yield following clear-cut logging in the Pacific Northwest,
826 *Water Resour. Res.*, 6, 653-658, 1970.
- 827 Sauer, V. B. and Meyer, R.W.:Determination of error in individual discharge measurements.
828 Open-File Report 92-144. U.S. Geological Survey, Norcross, Georgia, 1992.
- 829 Scanlon, B. R., Healy, R. and Cook, P.: Choosing appropriate techniques for quantifying
830 groundwater recharge, *Hydrogeol. J.*, 10, 91-109, 2002.
- 831 Scanlon, B. R., Christman, M., Reedy, R. C., Porro, I., Simunek, J. and Flerchinger, G. N.:
832 Intercode comparisons for simulating water balance of surficial sediments in semiarid regions,
833 *Water Resour. Res.*, 38, 59-1-59-16, doi:10.1029/2001WR001233, 2002.
- 834 Scibek, J. and Allen, D.: Modeled impacts of predicted climate change on recharge and
835 groundwater levels, *Water Resour. Res.*, 42, W11405, doi:10.1029/2005WR004742, 2006.
- 836 Shaw, R. H. and Pereira, A. R.: Aerodynamic roughness of a plant canopy: A numerical
837 experiment, *Agricultural Meteorology*, 26, 51-65, doi:10.1016/0002-1571(82)90057-7, 1982.
- 838 Smerdon, B., Mendoza, C. and Devito, K.: Influence of subhumid climate and water table
839 depth on groundwater recharge in shallow outwash aquifers, *Water Resour. Res.*, 44,
840 W08427, doi:10.1029/2007WR005950, 2008.
- 841 Sophocleous, M.: Quantification and regionalization of ground-water recharge in south-
842 central Kansas: integrating field characterization, statistical analysis, and GIS, *Spec Issue,*
843 *Compass*, 75, 101-115, 2000.
- 844 Stähli, M., Jansson, P. and Lundin, L. C.: Soil moisture redistribution and infiltration in
845 frozen sandy soils, *Water Resour. Res.*, 35, 95-103, 1999.

846 Vesala, T., Suni, T., Rannik, Ü, Keronen, P., Markkanen, T., Sevanto, S., Grönholm, T.,
847 Smolander, S., Kulmala, M. and Ilvesniemi, H.: Effect of thinning on surface fluxes in a
848 boreal forest, *Global Biogeochem. Cycles*, 19, GB2001, doi:10.1029/2004GB002316, 2005.

849 Vincke, C. and Thiry, Y.: Water table is a relevant source for water uptake by a Scots pine
850 (*Pinus sylvestris* L.) stand: Evidences from continuous evapotranspiration and water table
851 monitoring, *Agric. For. Meteorol.*, 148, 1419-1432, doi:10.1016/j.agrformet.2008.04.009,
852 2008.

853 Wang, Y., Woodcock, C. E., Buermann, W., Stenberg, P., Voipio, P., Smolander, H., Häme,
854 T., Tian, Y., Hu, J., Knyazikhin, Y. and Myneni, R. B.: Evaluation of the MODIS LAI
855 algorithm at a coniferous forest site in Finland, *Remote Sens. Environ.*, 91, 114-127,
856 doi:10.1016/j.rse.2004.02.007, 2004.

857 Westenbroeck, S. M., Kelson, V. A., Hunt, R. J. and Branbury, K.,R.: A modified
858 Thornthwaite-Mather Soil-Water-Balance code for estimating groundwater recharge, USGS,
859 Reston, Virginia, USA, 2010.

860 Wierenga, P., Hills, R. and Hudson, D.: The Las Cruces Trench Site: Characterization,
861 Experimental Results, and One-Dimensional Flow Predictions, *Water Resour. Res.*, 27, 2695-
862 2705, 1991.

863 Winter, T. C., Harvey, J. W., Franke, O. L. and Alley, W. M.: Ground water and surface
864 water; a single resource, USGS, Denver, Colorado, 79 pp., 1998.

865 Xiao, C., Janssens, I. A., Yuste, J. and Ceulemans, R.: Variation of specific leaf area and
866 upscaling to leaf area index in mature Scots pine, *Trees*, 20, 304-310, doi:10.1007/s00468-
867 005-0039-x, 2006.

868 Zaitsoff, O.: Groundwater balance in the Oripää esker, National Board of Waters, Finland,
869 Helsinki, 54-73 pp., 1984.

870 Zhou, Y.: A critical review of groundwater budget myth, safe yield and sustainability,
871 *J. Hydrol.*, 370, 207-213, doi:10.1016/j.jhydrol.2009.03.009, 2009.

872

873

874

875

876

877

878

879

880 **Tables**

881 **Table 1.** Characteristics of the study site annual climate.

VARIABLE	MEAN	STD
Precipitation [mm]	591	91
Air Temperature [°C]	-0.7	1.1
Reference ET [mm]	426	26

882

883 **Table 2.** Randomly varied parameters, related equations and parameter ranges included in the
884 model runs. For full description of parameters and equations, see Jansson and Karlberg (2004).

Parameter	Part of the model affected	Range	Units	Source
LAI (leaf area index)	Transpiration	0 ... 3.5	-	Data, see section 2.1.1
h (canopy height)	Transpiration	5 ... 15	m	Data
r_{alai} (increase in aerodynamic resistance with LAI)	Soil evaporation	25 ... 75	-	$\pm 50\%$, estimate
r_{ψ} (soil surface resistance control)	Soil evaporation	100...300	-	$\pm 50\%$ approximately to cover the surface resistance reported 150-1000 (Kelliher et al., 1998)
λ_L (pore size distribution index)	Soil evaporation, lichen	0.4 ... 1	-	Estimate, to cover an easily drainable range of pressure-saturation curves
Ψ_L (air entry)	Soil evaporation, lichen	1.5 ... 20	-	Estimate, to cover a easily drainable range of pressure-saturation curves
θ_L (porosity)	Soil evaporation, lichen	7.5...12.5	%	Data, lichen mean water retention $\pm SD$ from samples

$k_{mat,L}$ (matrix saturated hydraulic conductivity)	Soil evaporation, lichen	$5 \cdot 10^4 \dots 5 \cdot 10^7$	mm d^{-1}	Estimate, high K values assumed
t_{WD} (coefficient in the soil temperature response function)	Water uptake	10 ... 20	-	$\pm 50\%$, estimate
Ψ_c (critical pressure head for water uptake reduction)	Water uptake	200...600	-	$\pm 50\%$, estimate
$k_{mat,S}$ (matrix saturated hydraulic conductivity)	Soil profile	$1.707 \cdot 10^3 \dots 127.2 \cdot 10^3$	mm d^{-1}	Data from soil sample particle size analysis
k_{minuc} (minimum unsaturated hydraulic conductivity)	Soil profile	$1 \cdot 10^{-4} \dots 1 \cdot 10^{-1}$	mm d^{-1}	Estimate $k_{mat} * 1E-5$
λ_s (pore size distribution index)	Soil profile	0.4 ... 1	-	Range to cover measured pressure-saturation curves
Ψ_s (air entry)	Soil profile	20 ... 40	-	Range to cover measured pressure-saturation curves
θ_s (porosity)	Soil profile	0.25...0.36	%	Range from soil samples
θ_r (residual water content)	Soil profile	0.01...0.05	%	Range to cover measured pressure-saturation curves

885

886

887

888

889

890

891

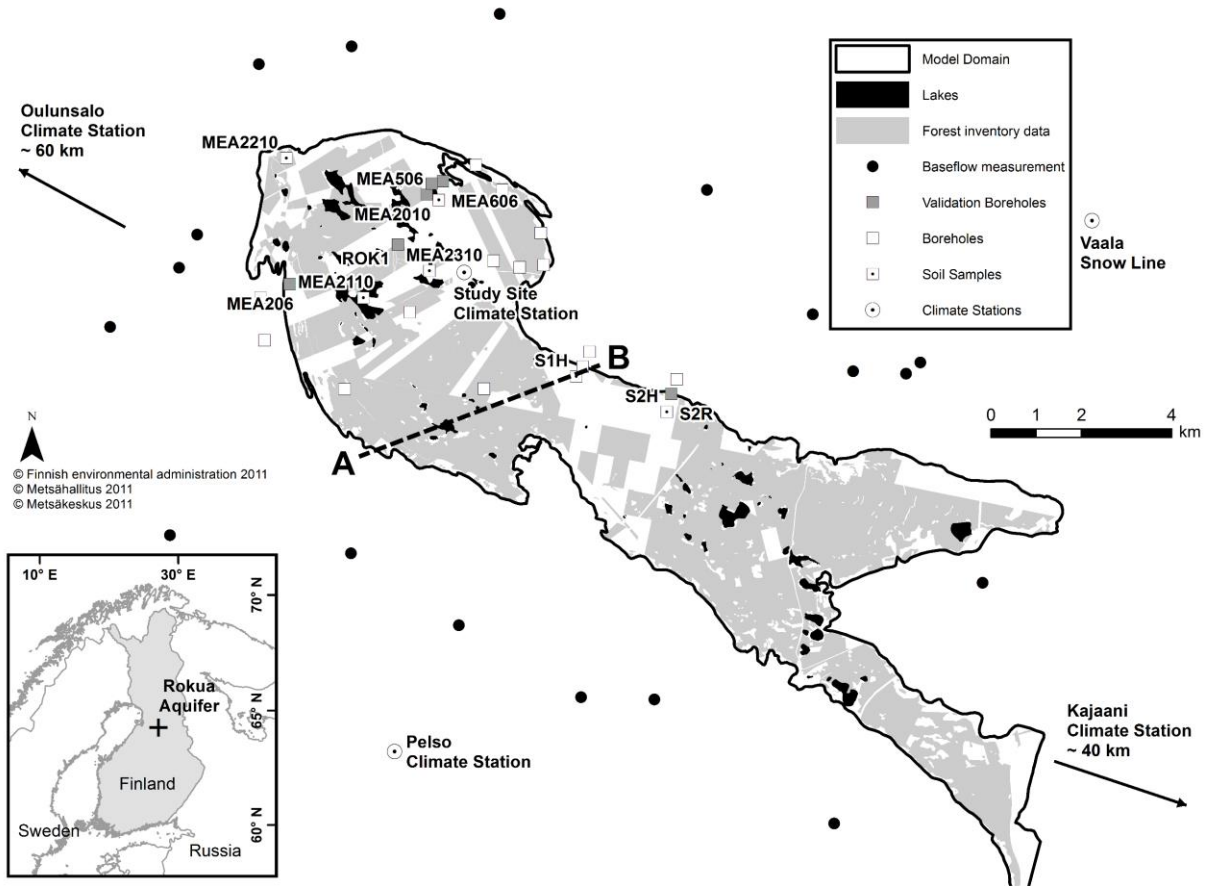
892

893 **Table 3.** Kendall correlation coefficient for simulation parameters and average annual sum of
 894 simulation output variables. ET = evapotranspiration, E = evaporation, for other symbols see
 895 Table 2.

Parameter	Total ET	Transpiration	Soil E	Snow E	Infiltration
LAI	0.59*	0.84*	-0.73*	-0.37*	0.18*
h	0.59*	0.84*	-0.73*	-0.37*	0.18*
r_{Ψ}	-0.11*	-0.03	-0.03	-0.61*	0.58*
r_{lai}	-0.13*	-0.02	-0.11*	0.03	-0.05
λ_L	-0.09*	-0.01	-0.11*	0.01	-0.03
Ψ_L	0.01	-0.04	0.11*	-0.04	0.06
θ_L	0.06	0.03	0.01	-0.00	0.09*
$k_{mat,L}$	-0.01	0.02	-0.04	-0.00	-0.00
$k_{mat,S}$	-0.10*	-0.04	-0.07*	0.02	0.01
k_{minuc}	-0.10*	-0.04	-0.07*	0.02	0.01
tWD	-0.05	-0.02	-0.03	-0.05	0.03
Ψ_c	0.18*	0.12*	-0.02	-0.04	0.05
λ_s	0.13*	0.06	0.06	-0.00	-0.23*
Ψ_s	-0.11*	-0.05	-0.04	-0.05	0.04
θ_s	0.02	-0.01	0.03	0.10*	-0.18*
θ_r	0.07*	0.05	-0.01	0.01	0.16*

896 *Significant correlation, $p < 0.05$

897



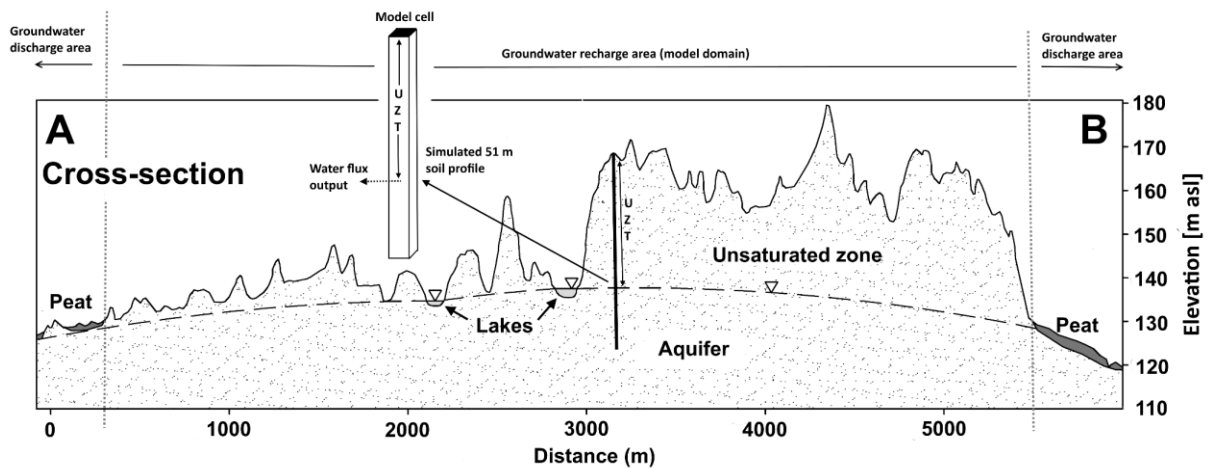
899

900 **Figure 1.** Recharge area of the Rokua esker aquifer. Boreholes in the area were used for model
 901 validation and soil type characterization. Baseflow was measured from streams originating
 902 outside the groundwater recharge area. Profile of cross-section A-B is presented in Fig. 2.

903

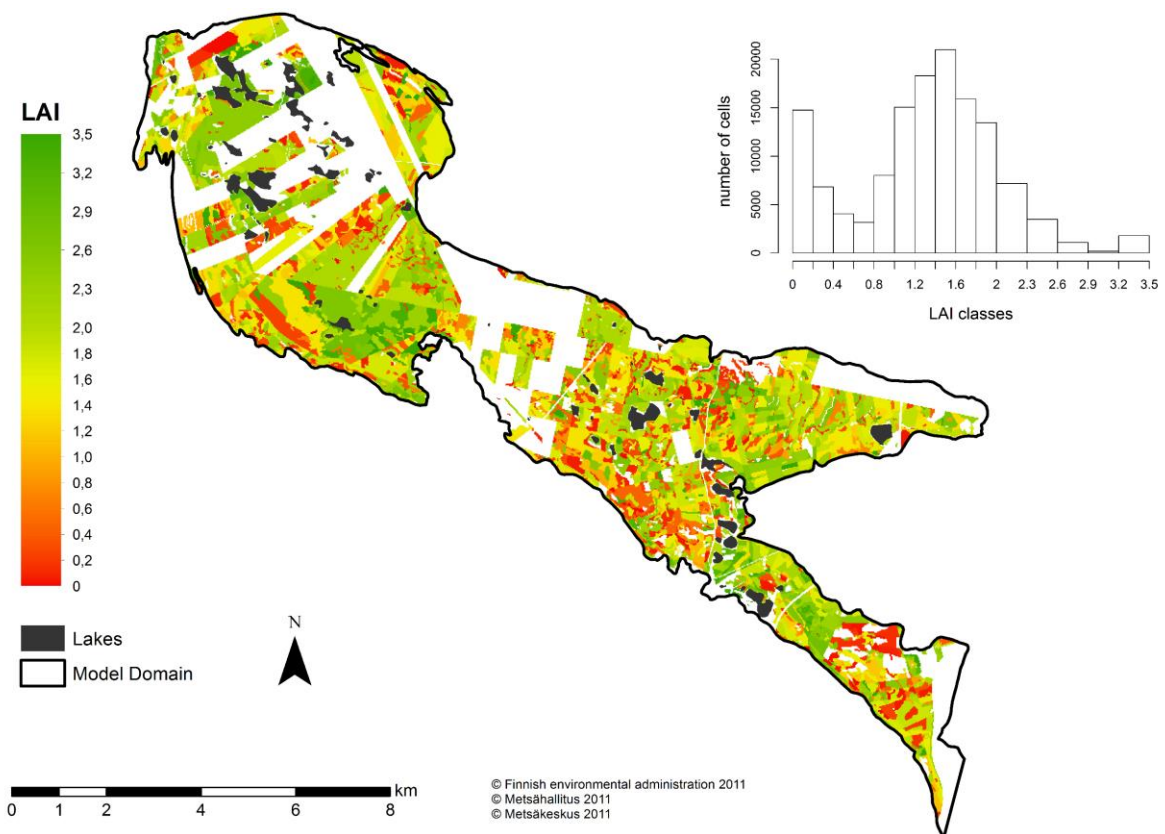
904

905



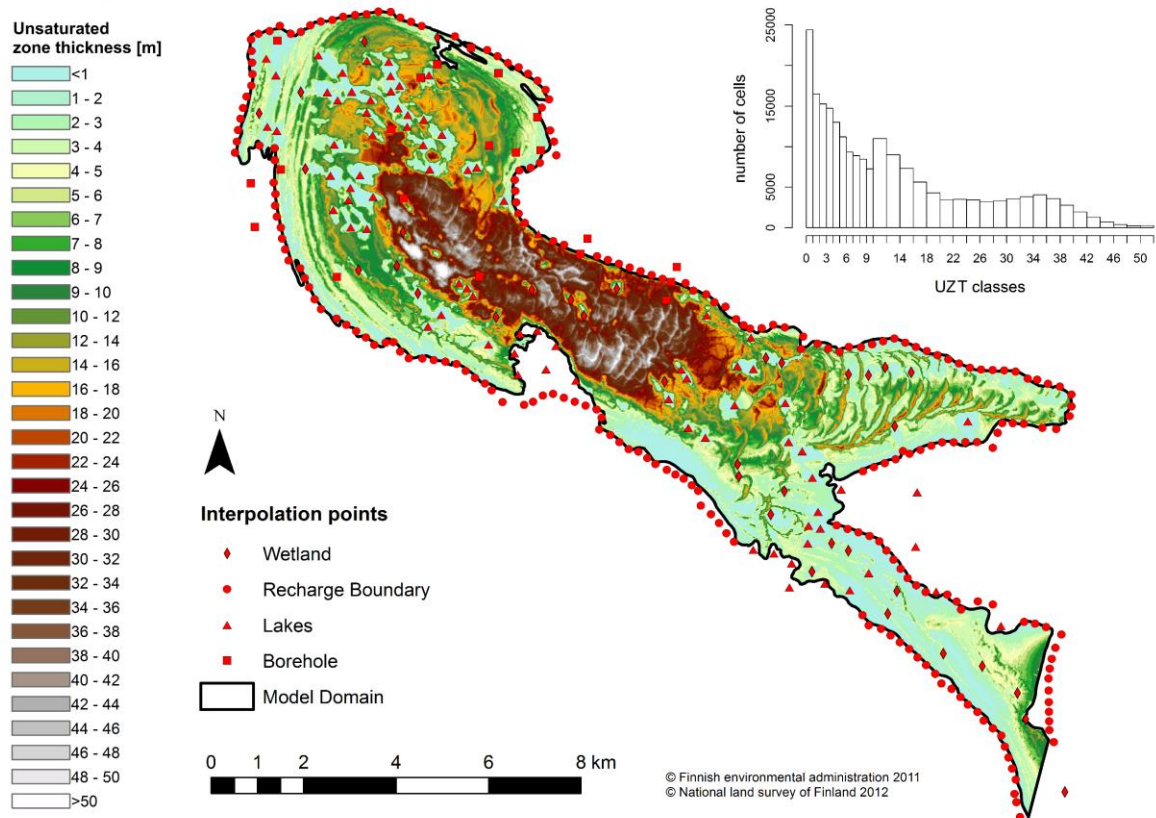
906

907 **Figure 2.** Cross-section A-B (Fig. 1) to demonstrate the geometry of the unsaturated zone and
 908 the aquifer (vertical axes exaggerated). A simulated soil profile is shown to give an example on
 909 how 1-D simulations are represented in the model domain, UZT represents the unsaturated zone
 910 thickness parameter.



911

912 **Figure 3.** Spatial distribution of leaf area index (LAI) and a 20m x 20m cell-based histogram
 913 of LAI values. In areas where forestry inventory data were lacking, a weighted average value
 914 of 1.25 was used in simulations.

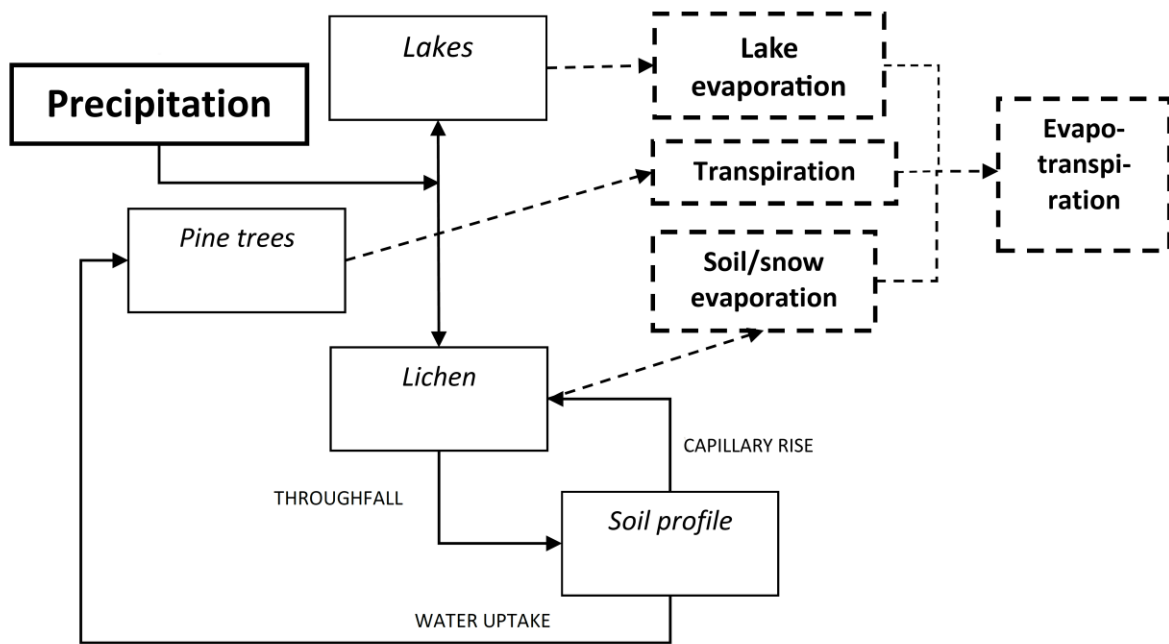


915

916 **Figure 4.** Estimated thickness of the unsaturated zone in the model area and interpolation points
 917 for estimation of water table elevation.

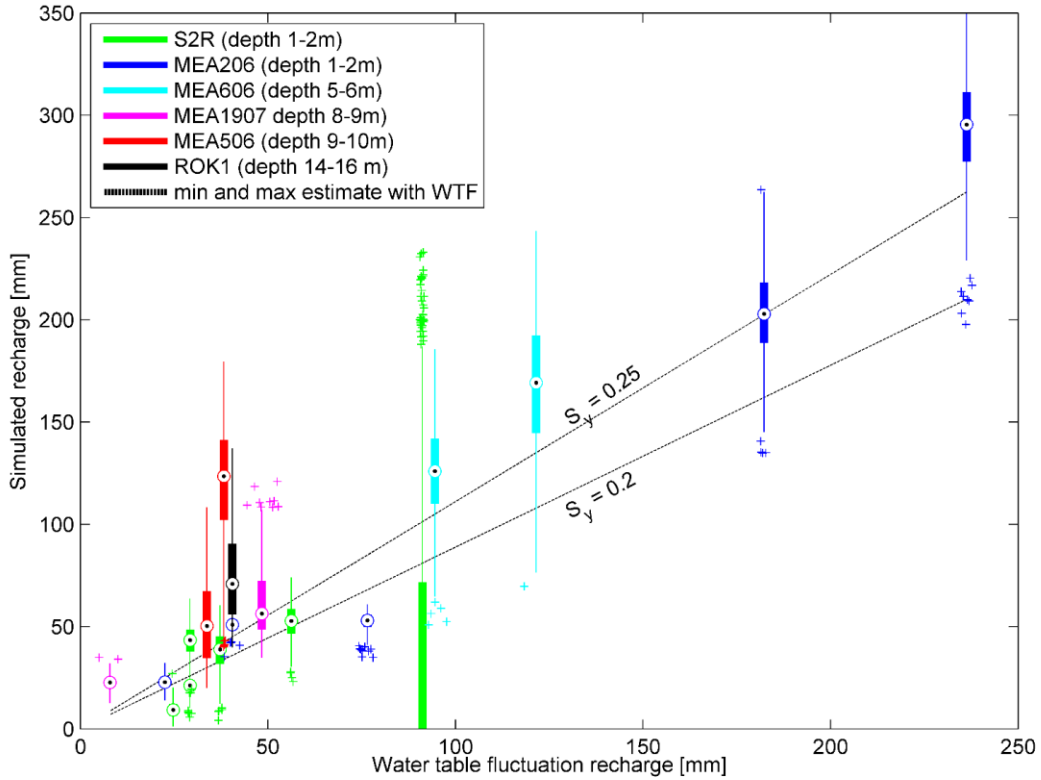
918

919



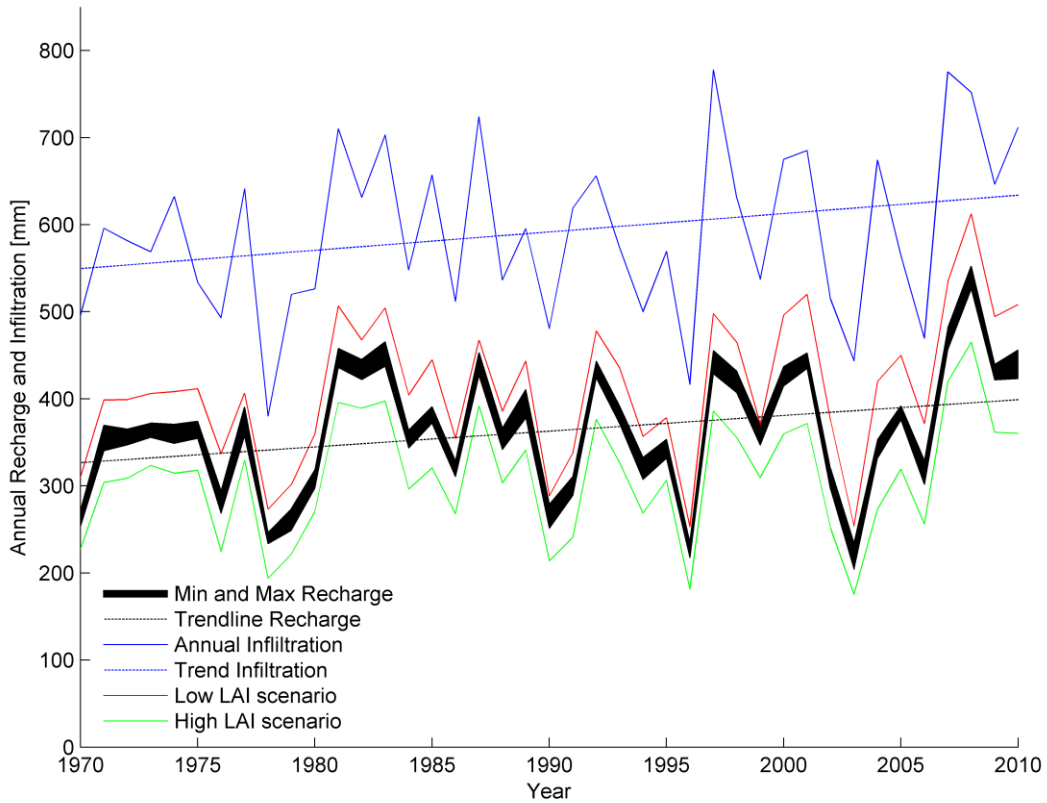
920

921 **Figure 5.** Flow chart of different evaporation processes considered in the study. Total
 922 evapotranspiration comprises of soil evaporation from the topmost soil layer, i.e. the lichen
 923 matrix, snow evaporation from snow surface, transpiration through the vascular system of tree
 924 canopy and lake evaporation from free water surface.



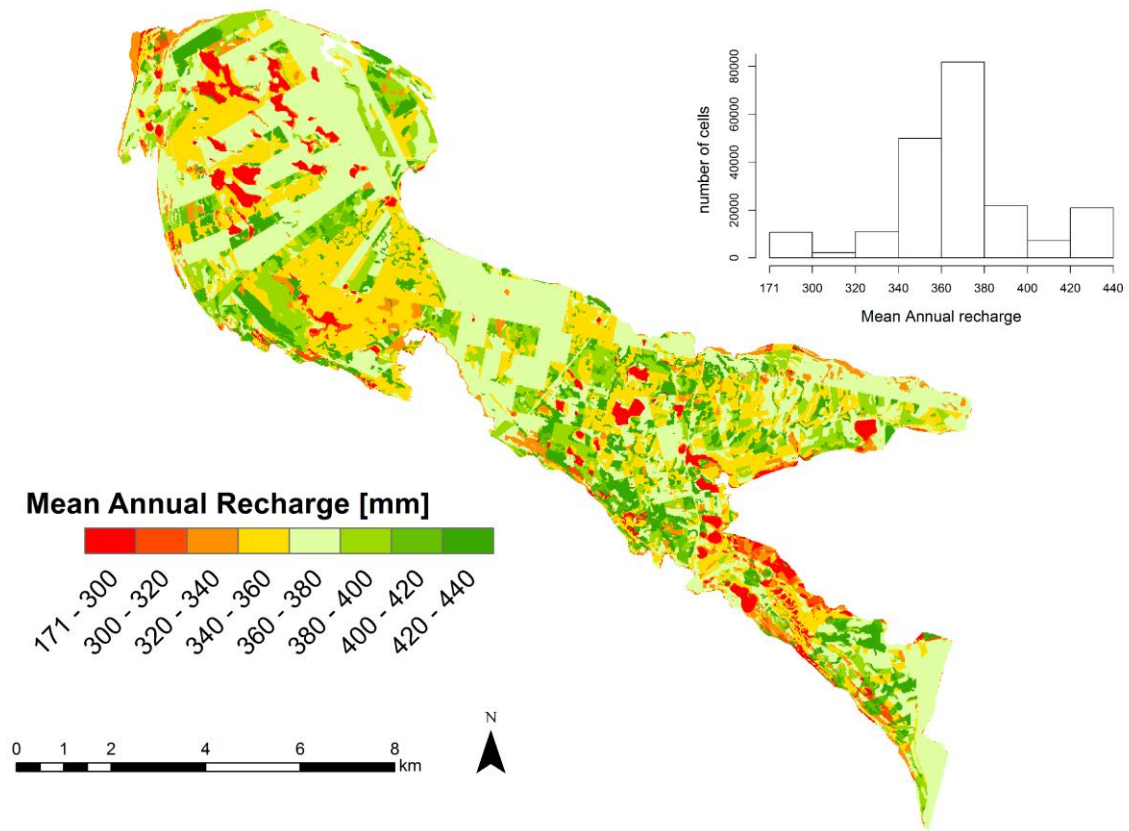
925

926 **Figure 6.** Assemblage of simulated recharge for individual recharge events, shown as boxplots
 927 where circles represent the median, bold lines 25-75th percentiles of the simulations, thin lines
 928 the remaining upper and lower 25th percentiles and crosses are outliers. The location of the
 929 boxplots on the x-axis is the WTF estimate for a given recharge event using a specific yield
 930 value of 0.225. The dashed lines indicate the uncertainty in the WTF estimates caused by the
 931 selection of specific yield. The two estimates would agree perfectly (given the uncertainty in
 932 S_y) if all simulations shown as boxplots fell between the dashed lines.



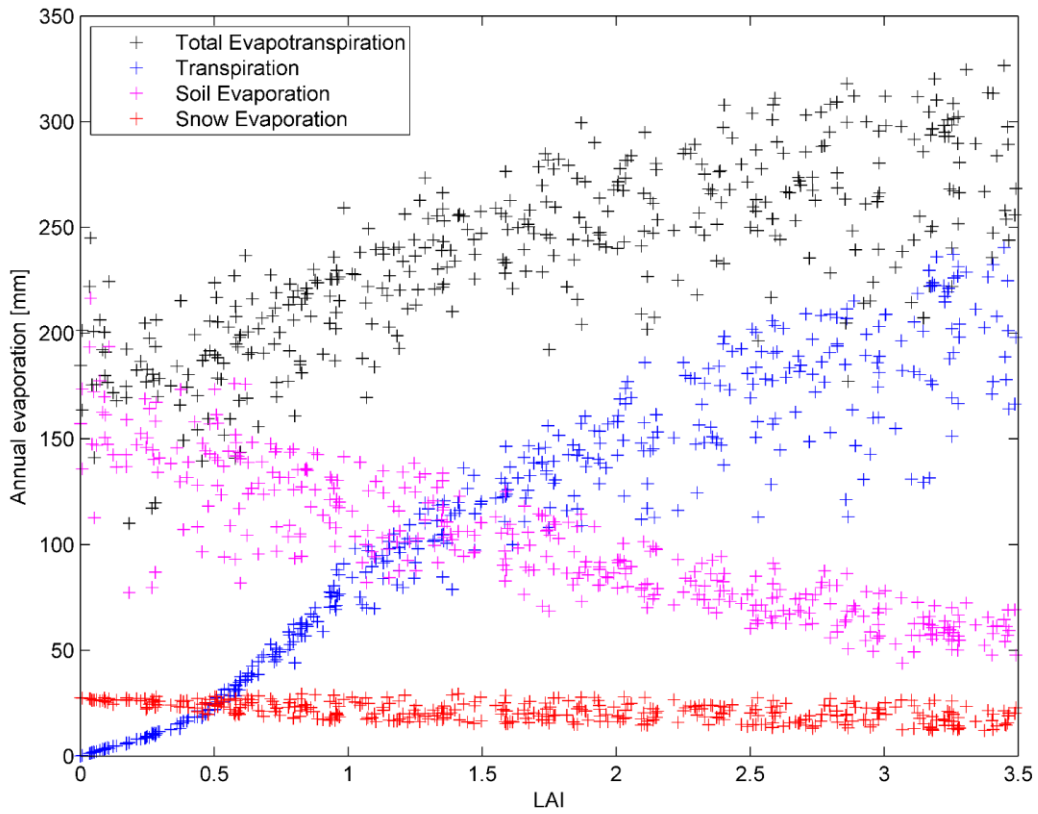
933

934 **Figure 7.** Annual recharge time series from simulations where the black area covers the
 935 minimum and maximum values for different recharge samples. The annual recharge pattern
 936 closely followed trends in infiltration. Effects of different land use management practices over
 937 time on annual recharge rates are shown as high and low leaf area index (LAI) scenarios.



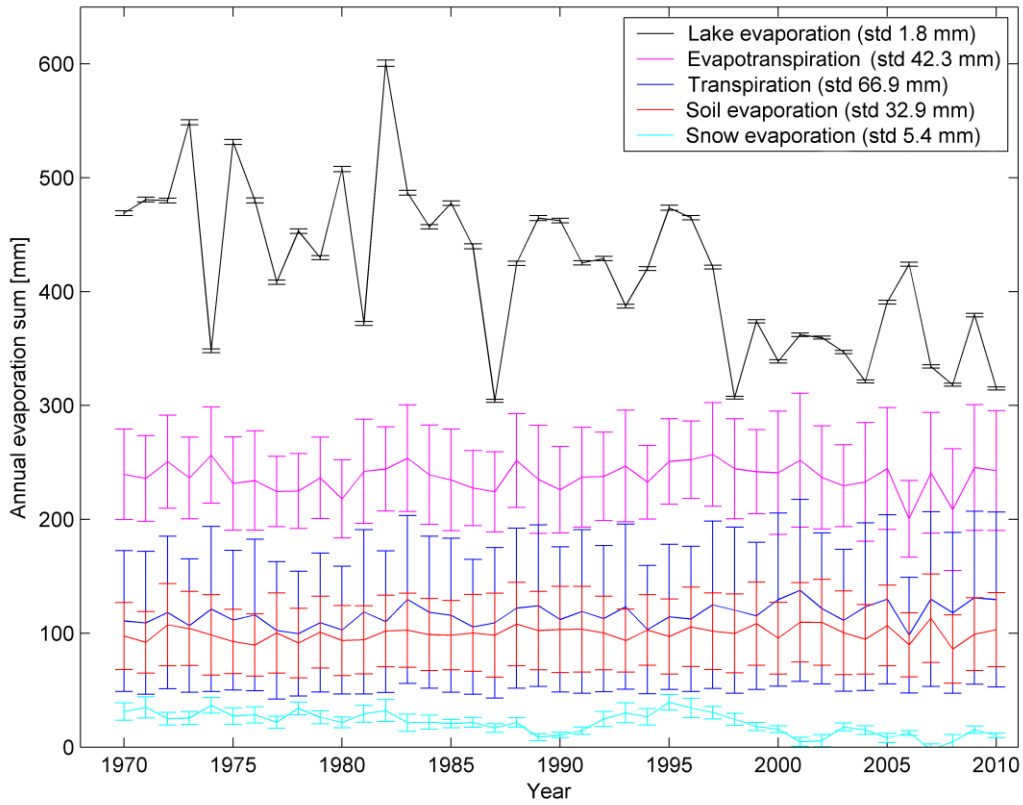
938

939 **Figure 8.** Spatial distribution of mean annual recharge, which was influenced mainly by the
 940 Scots pine canopy (LAI), the presence of lakes and, to some extent, areas with a shallow water
 941 table.



942

943 **Figure 9.** Example of scatter plots with the mean annual ET components are plotted as a
944 function of the variable leaf area index (LAI), showing clear dependence of all ET components
945 on LAI.



946

947 **Figure 10.** Values of different evapotranspiration (ET) components (mean and standard
 948 deviation) simulated for the study period.